

RESTRICTED UNCLASSIFIED
CONFIDENTIAL

Copy No. 6
RM No. L8H04

NACA RM No. L8H04

2 NOV 1948

CLASSIFIED

NACA

RESTRICTED

naca Release form #639

H.L. Dryden, et al. July 3/1957

RESEARCH MEMORANDUM

by HGR, 8-2-51

AERODYNAMIC CHARACTERISTICS OF TWO ALL-MOVABLE WINGS TESTED
IN THE PRESENCE OF A FUSELAGE AT A MACH NUMBER OF 1.9

By

D. William Conner

Langley Aeronautical Laboratory
Langley Field, Va.

CLASSIFICATION CANCELLED

CLASSIFIED DOCUMENT

This document contains classified information affecting the National Defense of the United States within the meaning of the Espionage Act, USC 50:31 and 32. Its transmission or the revelation of its contents in any manner to an unauthorized person is prohibited by law. Information so classified may be imparted only to persons in the military and naval services of the United States, appropriate civilian officers and employees of the Federal Government who have a legitimate interest therein, and to United States citizens of known loyalty and discretion who if necessary must be informed thereof.

J.W. Crowley Date 12/7/53
J.E.C. 10501
MHA 12/12/53 See NACA
R 7 1634

NATIONAL ADVISORY COMMITTEE FOR AERONAUTICS

WASHINGTON
October 28, 1948

NACA LIBRARY
LANGLEY MEMORIAL AERONAUTICAL
LABORATORY
Langley Field, Va.

CONFIDENTIAL

RESTRICTED

UNCLASSIFIED



UNCLASSIFIED

NATIONAL ADVISORY COMMITTEE FOR AERONAUTICS

RESEARCH MEMORANDUM

AERODYNAMIC CHARACTERISTICS OF TWO ALL-MOVABLE WINGS TESTED

IN THE PRESENCE OF A FUSELAGE AT A MACH NUMBER OF 1.9

By D. William Conner

SUMMARY

Half-span models of two wings of different plan form were tested both as all-movable surfaces and as fixed surfaces in the presence of a half fuselage in the Langley 9- by 12-inch supersonic blow-down tunnel at a Mach number of 1.9. One wing had a half-delta plan form with 60° leading-edge sweep and was tested at a Reynolds number of 1.9×10^6 . The other wing had a rectangular plan form modified by an Ackeret type tip and was tested at a Reynolds number of 1.4×10^6 . Both surfaces operated well within the Mach cone originating at the fuselage nose. The circular cross sections of the fuselage were modified to provide a flat area in the region of the wing root.

A comparison of the data indicated that either wing acting as an all-movable surface would have about the same spanwise and chordwise location of the center of pressure as the same wing acting as a fixed surface, but the fixed-surface arrangement would have a lift-curve slope about 30 percent greater than the wing-free (all-movable) arrangement. The change in upwash represented by this increase in lift-curve slope is in good agreement with calculations based on a method recommended by L. Beskin.

INTRODUCTION

All-movable aerodynamic surfaces are being considered in supersonic aircraft design for possible applications as angle-of-attack indicators, control surfaces, and all-movable wings. Present methods used in calculating the supersonic characteristics of such surfaces operating in the presence of a fuselage must resort to several simplifying assumptions, especially if the fuselage contour is modified to minimize the junction gaps caused by surface rotation. In order to obtain experimental data for all-movable surface arrangements, half-span models of two wings of different plan form were tested both as all-movable surfaces and as conventional fixed surfaces in the presence of a half fuselage in the Langley 9- by 12-inch supersonic blow-down tunnel.

~~CONFIDENTIAL~~

UNCLASSIFIED

One wing had a 60° sweptback half-delta plan form and 9-percent-thick circular-arc sections. The other wing had a trapezoidal plan form, formed by a rectangular wing modified by an Ackeret type wing tip and had 10-percent-thick double-wedge sections. A small area on the fuselage at the wing-fuselage juncture was flat and parallel with the air stream to prevent a change in the end gap when the wing rotated on the fuselage. Lift, drag, pitching moment, and rolling moment were obtained at a

Mach number of 1.9 and a Reynolds number of about 1.9×10^6 for the delta wing and 1.4×10^6 for the trapezoidal wing.

SYMBOLS

C_L	lift coefficient based on area of exposed surface
C_D	drag coefficient based on area of exposed surface
C_m	pitching-moment coefficient based upon the mean aerodynamic chord of exposed model surface and computed about the 50-percent-chord point of the mean aerodynamic chord (center of area)
C_l	rolling-moment coefficient based on twice the area of the exposed aerodynamic surface and on a span b
α	wing angle of attack, measured with respect to the free-stream direction
M	free-stream Mach number
R	Reynolds number based on the mean aerodynamic chord of the exposed aerodynamic surface
b	twice the distance from the fuselage axis to the wing tip
\bar{c}	mean aerodynamic chord of the exposed model surface
Δp	increment in pressure
q	free-stream dynamic pressure

MODELS

Photographs of the two semispan models are shown in figure 1. The principal dimensions of the two aerodynamic surfaces, hereafter called wing panels, and the fuselage are shown in figure 2. Both wing panels and the fuselage are fabricated from aluminum and have a polished finish.

As shown in figure 2(a), the first wing panel has a half-delta plan form with 60° sweepback of the wing leading edge. The airfoil sections taken parallel to the air stream are symmetrical circular-arc profiles 9 percent thick. The aspect ratio of this plan-form delta wing is 2.31. The wing panel is rotated about the 60-percent point of the wing root chord which is slightly ahead of the center of area.

The second wing panel, for which details are shown in figure 2(b), has an unswept trapezoidal plan form formed by a rectangular wing modified by an Ackeret type wing tip to relieve the wing area of tip Mach cone effects. The airfoil sections taken parallel to the air stream are symmetrical double-wedge profiles 10 percent thick. The aspect ratio of this wing, including the extension through the fuselage, is 4.12. The wing panel is rotated about the midchord point of the wing root chord which is slightly behind the center of area.

The fuselage used in these tests is a half body of revolution (having a parabolic profile) split lengthwise along the axis as shown in figure 1. In the region of maximum thickness where the wing panels are located, the fuselage contour has been modified by a flat area formed by cutting the fuselage body of revolution with a plane parallel to the body axis and perpendicular to the wing axis of rotation. This flat has a maximum width of 0.80 inch, which permits the wing to be rotated through a small angle range without the appearance of an appreciable gap between the wing and fuselage. The wing root is mounted on the balance through a disk 0.80 inch in diameter set flush with the fuselage flat but not touching the fuselage. Under no load a radial gap of 0.010 inch is maintained all around the disk and a gap of 0.005 inch is maintained between the overhanging portion of the wing and the fuselage flat. The 0.005 gap is not sealed for any of the tests. The deflections caused by the aerodynamic loads on the model are the limiting factor of the angle-of-attack range.

TUNNEL AND TEST TECHNIQUE

The Langley 9- by 12-inch supersonic blow-down tunnel in which the present tests were made is a nonreturn-type tunnel, utilizing the exhaust air of the Langley 19-foot pressure tunnel. Free-stream Mach number is 1.90. The air enters at an absolute pressure of about $2\frac{1}{3}$ atmospheres and contains about 0.003 pound of water per pound of air.

The semispan models used in these tests are cantilevered from the tunnel wall. This arrangement provides a simple, rigid means for mounting the models and permits the scale of the models to be large in relation to the size of the test section.

Preliminary tests indicated that wings cantilevered directly from the tunnel floor would be operating in a boundary layer about 0.4 inch thick. The possibility of testing half-span wings in the presence of a fuselage was next explored since any practical supersonic configuration would include a fuselage. In the ideal arrangement, the flow field over the fuselage mounted on the tunnel wall would duplicate the flow field over a fuselage located in the center of the jet. A complete fuselage was mounted parallel with the wind stream in the center of the tunnel and surveys were made of the surface pressures and of the boundary-layer profile in the region where the wing would be located. The fuselage was then split lengthwise and the half fuselage was mounted on the tunnel wall where similar measurements were made. The results shown in figure 3 indicated that the fuselage boundary layer was thicker when the fuselage was on the wall. Various thickness shims were tried as a fairing between the half fuselage and the wall in order to move the fuselage out of the wall boundary layer. As the fuselage was moved out from the wall, the fuselage boundary-layer thickness decreased and, with a 0.25-inch shim, very closely approached that measured on the complete fuselage in the center of the jet. Shimming the fuselage away from the wall also brought the pressure distribution along the fuselage in better agreement with that measured in the center of the tunnel. The surveys were made only with the fuselage aligned with the wind stream, and the comparison might be somewhat different for other fuselage attitudes. From these results, it appeared satisfactory to test wings in the presence of this half fuselage shimmed out 0.25 inch from the tunnel wall, and such a technique was used in these wing tests. (In examining the survey results shown in figure 3 only qualitative comparisons should be made since quantitative errors might exist. This is true of the pressure distribution because of the limited range of surveyed static pressures along the tunnel. Such errors might exist in the shape of the boundary-layer profile because the 0.030-inch-outside-diameter total-pressure tube was relatively large when compared with the boundary-layer thickness.)

The semispan model cantilevered from the tunnel wall is attached to a four-component electric-strain-gage balance. The balance rotates with the model and measures pitching moment, chord force, normal force, and rolling moment due to normal force. The rolling-moment coefficient is therefore measured about an axis lying in the wing-chord plane, but for small angles of attack, it closely approximates the rolling-moment coefficient about the wind axis. Forces on the body were not measured in any of the tests.

It should be pointed out that several factors, not as yet fully investigated, might influence the test results obtained in this tunnel. Several of these factors are:

- (1) Air loading might be carried over that part of the model located inside the fuselage. A few pressure measurements obtained on a different wing from those used in these tests indicated this loading to be quite small but still measurable.

(2) Stray shock waves of marked intensity might be present in the test-section region. Such waves might well have been missed during the tunnel calibration in which a pattern of readings was obtained from pressures on several cones, a wedge and behind the normal shock of a total-pressure tube. No schlieren equipment has been provided for visual observations.

(3) Condensation, resulting from the high moisture content of the inlet air, has been considered as having possible effects on aerodynamic results, particularly pitching moment and the characteristics of control surfaces.

With regard to items (2) and (3), it might be well to mention that unreported aileron-effectiveness tests of a sweptback wing model in this tunnel showed very good agreement with free-flight rocket tests of a similar wing-aileron configuration.

The dynamic pressure and test Reynolds number decreased about 5 percent during the course of each run because of the decreasing pressure of the inlet air. The average dynamic pressure for these tests was 1670 pounds per square foot and the average Reynolds number was 1.9×10^6 for the half-delta wing panel and 1.4×10^6 for the unswept wing panel.

PRECISION OF DATA

Free-stream Mach number has been calibrated at 1.90 ± 0.02 . This Mach number was used in determining the dynamic pressure. The variation of the static pressure with the tunnel clear varied about ± 1.5 percent in the test-section region.

The accuracy of measurements is indicated in the following table:

Variable	Error
α	$\pm 0.05^\circ$
C_L	.005
C_D	.001
C_m	.001
C_z	.002

Repeat tests were made for each configuration and, in fairing the curves, those tests were favored which had smaller zero shifts of the balance readings. The rolling-moment component was especially sensitive to shifts in wind-off readings. The faired curves should be more accurate than the table indicates.

RESULTS AND DISCUSSION

The experimental characteristics of the two wings are presented in figures 4 and 5 and the lift-drag ratios calculated from the faired curves of figures 4 and 5 are presented in figure 6. Some of the important results are summarized in table I.

Lift characteristics.— From table I, it may be seen that the wing-fixed arrangement increased the lift-curve slope by about 30 percent over the wing-free (or all-movable) arrangement. The values were increased from 0.038 to 0.050 for the trapezoidal wing and from 0.029 to 0.040 for the delta wing. The wing-free values were the same when the fuselage was either aligned with the wind stream or was positioned at an attitude of 4° . Fuselage upwash was calculated for these two wing-fuselage combinations by the method recommended in reference 1. Since this method considers fuselages having only circular cross sections, the following assumptions were made to account for the flattened area on the fuselage used in these tests:

(1) At the wing root the upwash was assumed to be that calculated for a smaller-diameter fuselage having a surface tangent to the wing root.

(2) At increasing distances from the fuselage surface, the upwash was assumed to approach that of the basic fuselage without the flattened area. The spanwise upwash variation would then be represented by a smooth transition from the upwash variation of the assumed smaller fuselage at the wing root to the upwash variation of the basic fuselage at a distance of one fuselage diameter from the wing root.

The calculations indicated that the upwash field introduced by changing the fuselage angle of attack would effectively increase the angle of attack of wings of either plan form by about 30 percent. This large upwash effect which is a result of the small size of the wings relative to the fuselage diameter accounts for the difference in lift-curve slopes between the wing-free and wing-fixed test results.

In two instances with the wing free, the nose of the delta wing was no longer on the fuselage flat and a discontinuity existed. This discontinuity occurred when the wing angle of attack exceeded 8° for the fuselage fixed at zero angle and also when the wing angle of attack was more negative than -4° for the fuselage positioned at a 4° angle of attack.

There was no evidence of a force break for these conditions although the fuselage boundary layer might have been thick enough to conceal any possible effects.

Center of pressure.-- From the slopes of the lift curves, rolling-moment curves, and pitching-moment curves, both the spanwise and chordwise locations of the center of pressure have been calculated and are tabulated in table I. Freeing the wing from the fuselage caused only slight shifts in the location of the center of pressure, the spanwise location moving out about 0.01b for both wings, and the chordwise location moving ahead for the trapezoidal wing and moving back for the delta wing. This movement was small, the forward shift for the trapezoidal wing being 0.007c and the rearward movement for the delta wing being 0.015c. The spanwise locations of the center of pressure were about on the centers of area and the chordwise locations were from 0.05c to 0.10c ahead of the centers of area.

Drag.-- By use of the method of reference 2, the wave-drag coefficients of the delta and trapezoidal wings were calculated to be 0.023 and 0.025, respectively, for a Mach number of 1.9. Adding to these a skin-friction drag coefficient of 0.006 brought the results in reasonable agreement with the experimental values of minimum drag listed in table I. Freeing the wing from the fuselage caused little difference in minimum drag but did cause a considerable decrease in the maximum values of the lift-drag ratio when the fuselage was aligned with the air stream. Such calculations of lift-drag ratio are, however, incomplete since the drag of the fuselage is not included.

CONCLUDING REMARKS

From tests of two semispan wings of different plan form operating in the presence of a half fuselage at a Mach number of 1.9, a comparison has been made of the results where the fuselage and wing rotated congruently with the results where the fuselage was restrained at a fixed angle and the wing was allowed to rotate. The data indicated that either wing acting as an all-movable surface would have about the same spanwise and chordwise location of the center of pressure as the same wing acting as a fixed surface but the fixed-surface arrangement would have a lift-curve slope about 30 percent greater than the wing-free (or all-movable) arrangement. The change in upwash represented by this decrease in lift-curve slope is in good agreement with theory.

Langley Aeronautical Laboratory
National Advisory Committee for Aeronautics
Langley Field, Va.

[REDACTED]

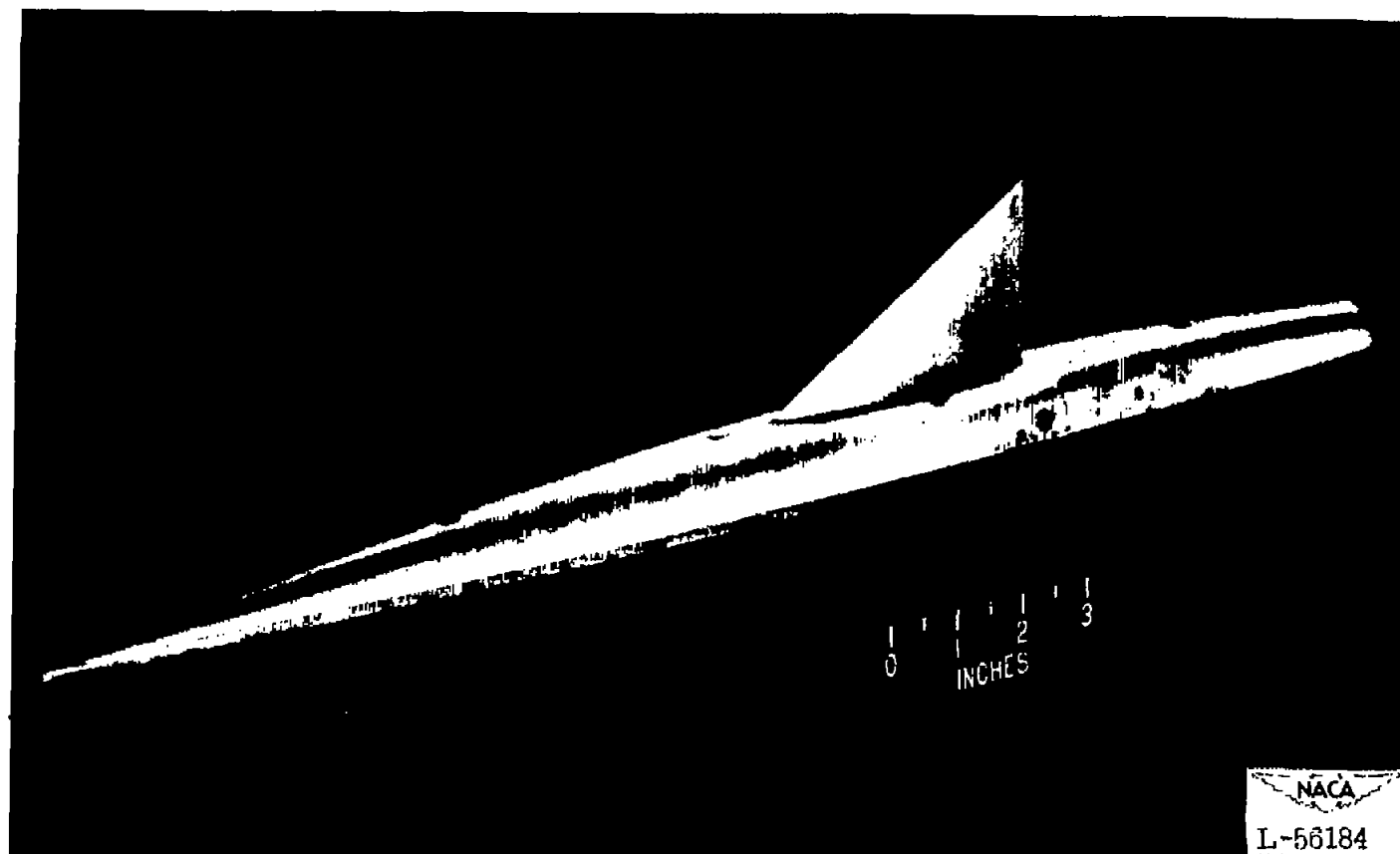
REFERENCES

1. Beskin, L.: Determination of Upwash around a Body of Revolution at Supersonic Velocities. CVAC-DEVF Memo. BB-6, APL/JHU-CM-251 The Johns Hopkins Univ., Appl. Phys. Lab., May 27, 1946.
2. Puckett, Allen E.: Supersonic Wave Drag of Thin Airfoils. Jour. Aero. Sci., vol. 13, no. 9, Sept. 1946, pp. 475-484.

TABLE I
EXPERIMENTAL CHARACTERISTICS OF WINGS

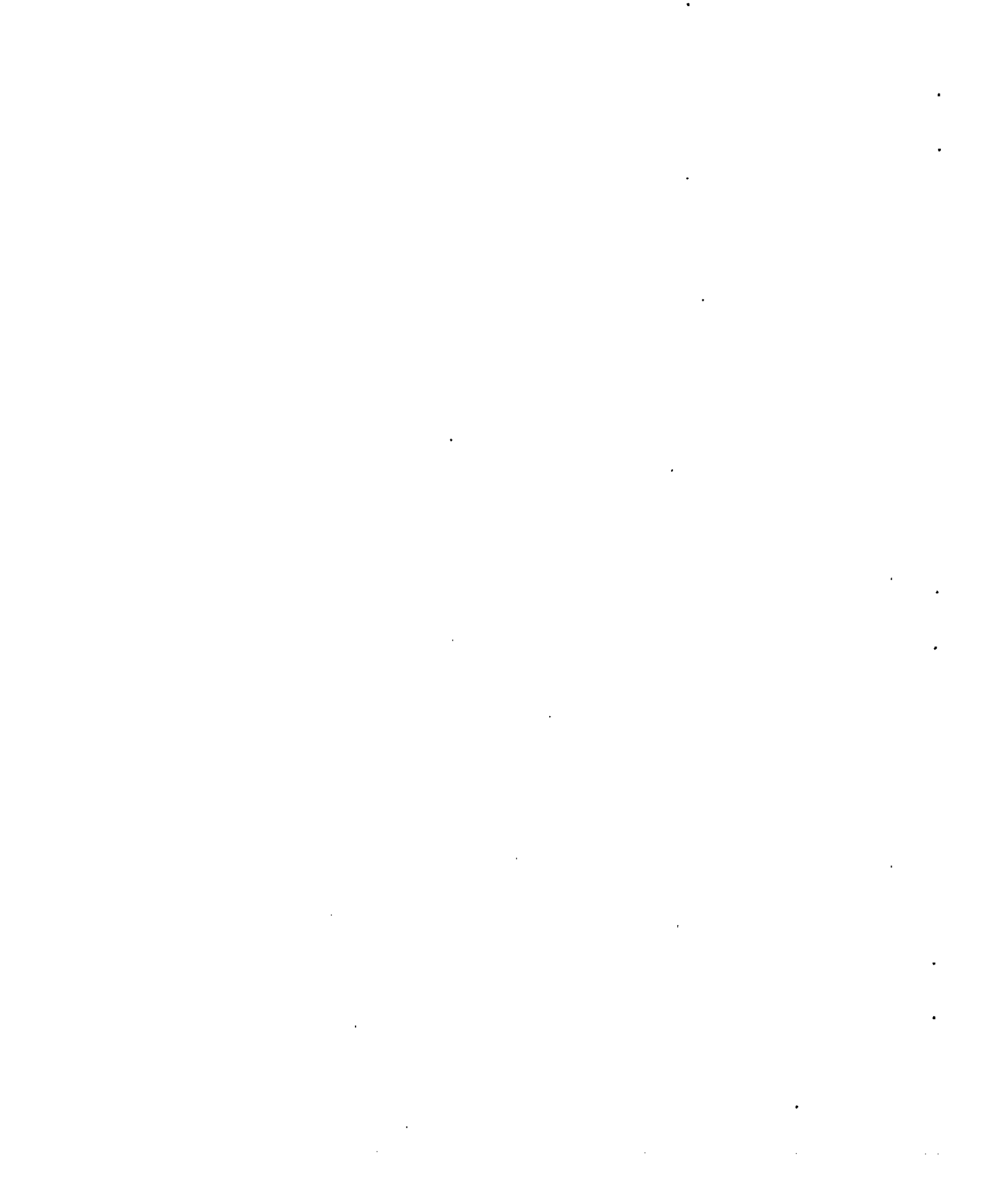
	Trapezoidal Wing			Delta Wing		
	Wing fixed (rotating with fuselage)	Wing-free fuselage at -		Wing fixed (rotating with fuselage)	Wing-free fuselage at -	
		0°	4°		0°	4°
$dC_L/d\alpha$	0.050	0.038	0.038	0.040	0.029	0.029
$dC_l/d\alpha$	0.0061	0.0048	0.0048	0.0051	0.00385	0.00385
$dC_m/d\alpha$	0.0045	0.0037	0.0037	0.0027	0.0015	0.0015
$C_{D_{min}}$	0.030	0.030	0.030	0.027	0.027	0.027
L/D_{max}	4.4	4.1	4.4	5.0	4.1	4.7
Spanwise location of center of pressure from fuselage center line, fraction of b	.244	.252	.252	.255	.265	.265
Chordwise location of center of pressure ahead of wing center of area, fraction of \bar{c}	.090	.097	.097	.067	.052	.052

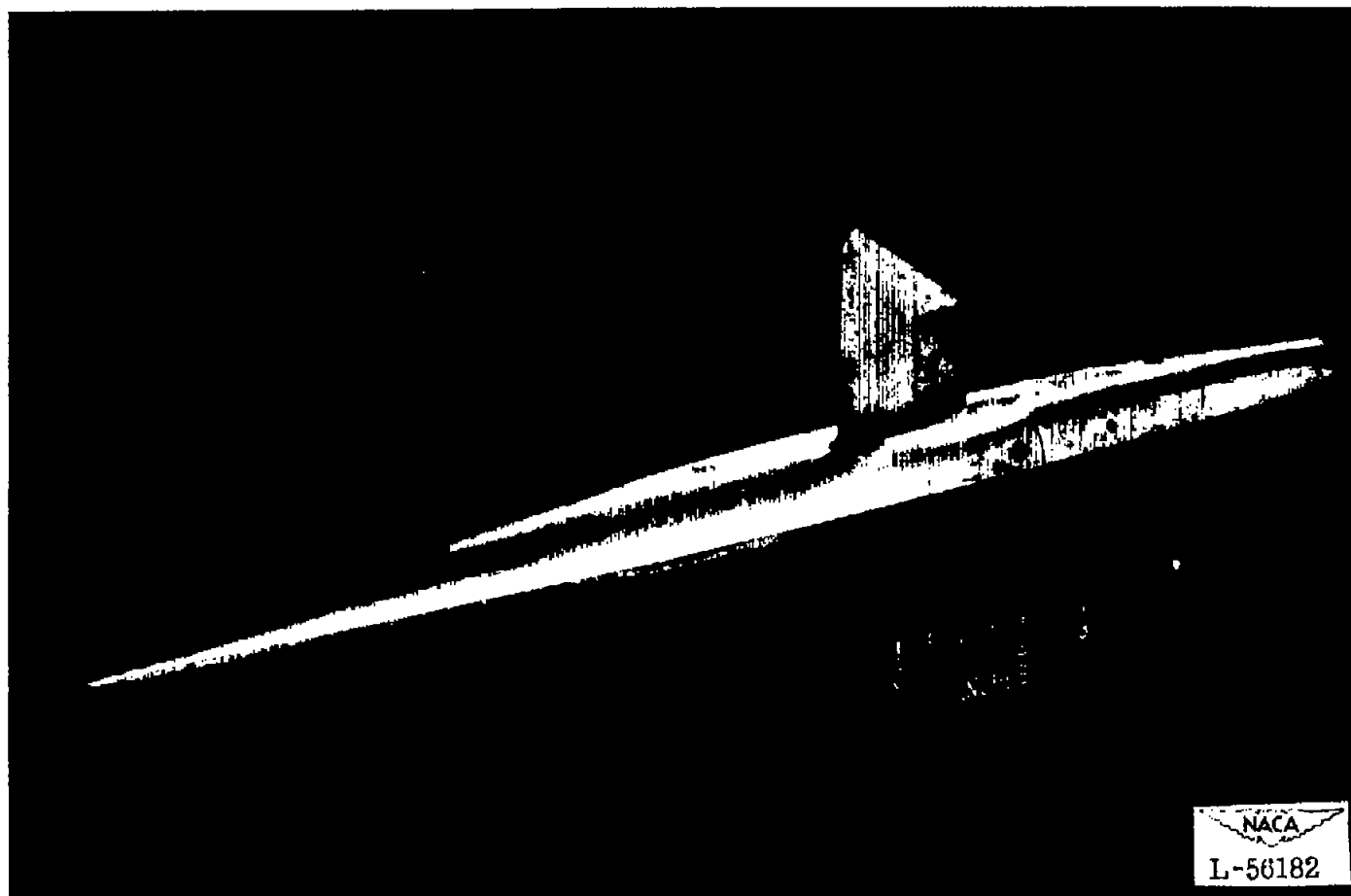

 NACA



(a) Delta wing.

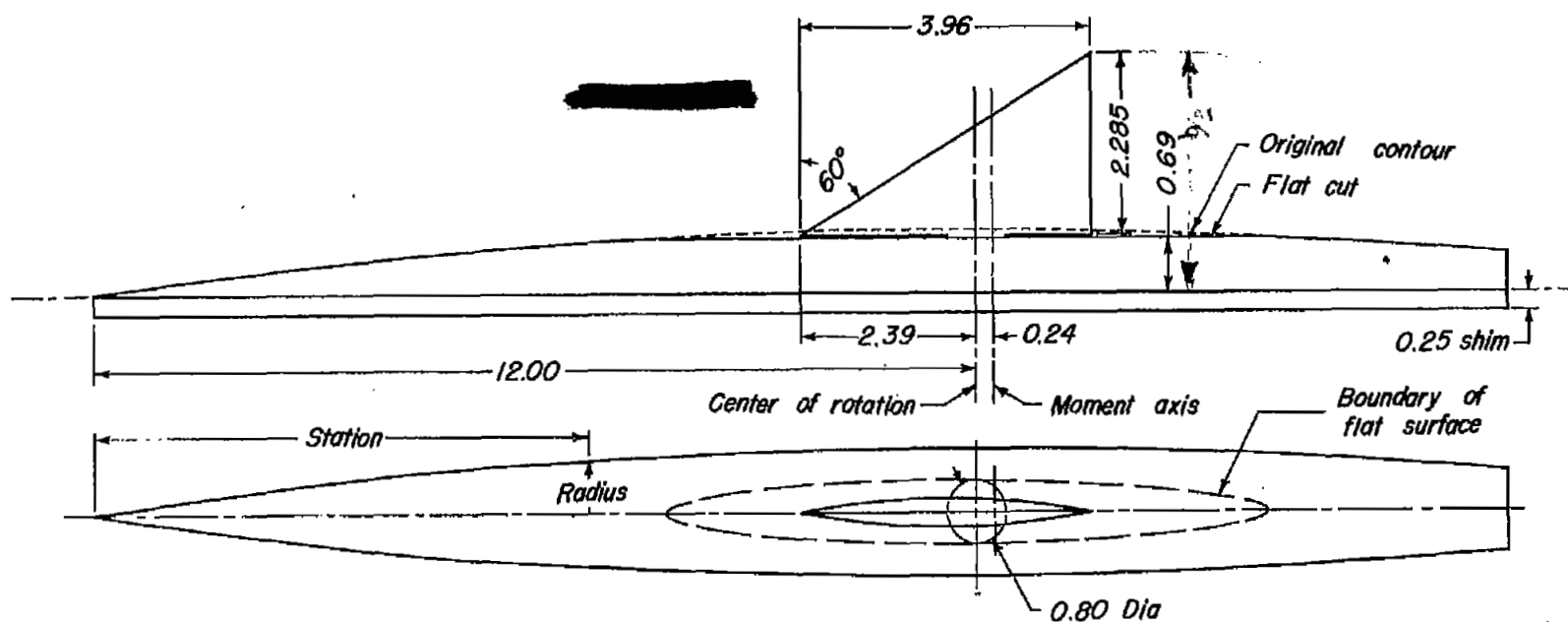
Figure 1.- Photographs of wing-fuselage combinations.





(b) Trapezoidal wing.

Figure 1.- Concluded.



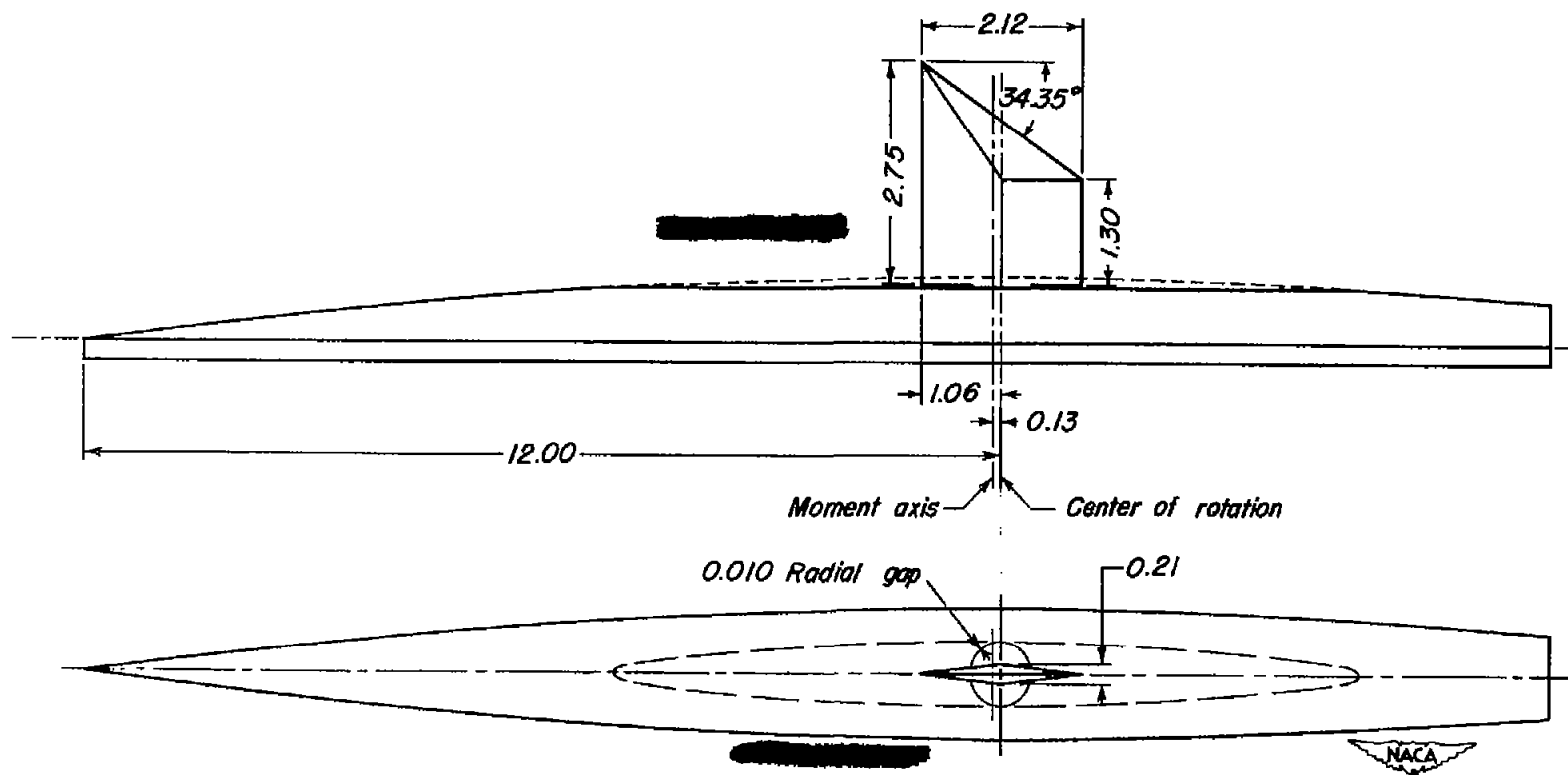
Fuselage ordinates			
Station	Radius	Station	Radius
0	0	11.20	0.796
.80	.103	12.00	.800
2.00	.244	12.80	.796
3.20	.370	13.60	.786
4.40	.479	14.80	.756
5.60	.572	16.00	.711
6.80	.650	17.20	.650
8.00	.711	18.40	.572
9.20	.756	19.20	.512
10.40	.786		

Wing ordinates (in percent chord)			
Station	Ordinate	Station	Ordinate
0	0	0	0
11.4	± 1.8	59.7	± 4.3
21.0	3.0	69.4	3.8
30.9	3.8	79.0	3.0
40.3	4.3	88.6	1.8
50.0	4.5	100.0	0.



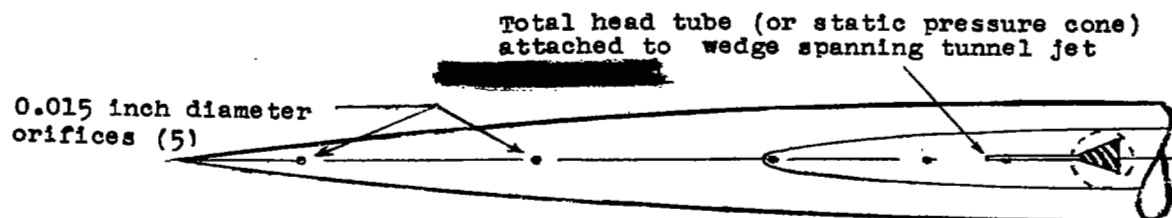
(a) Delta wing; mean aerodynamic chord = 2.64; span = 5.95.

Figure 2.- Details of wings and fuselage. All dimensions in inches.

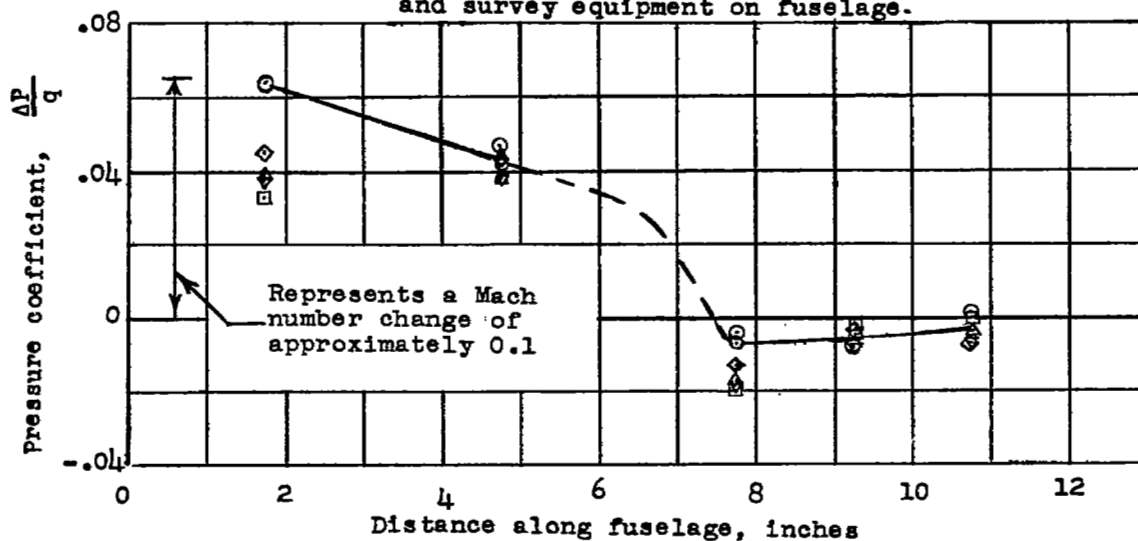


(b) Trapezoidal wing; mean aerodynamic chord = 1.867; span = 6.88.

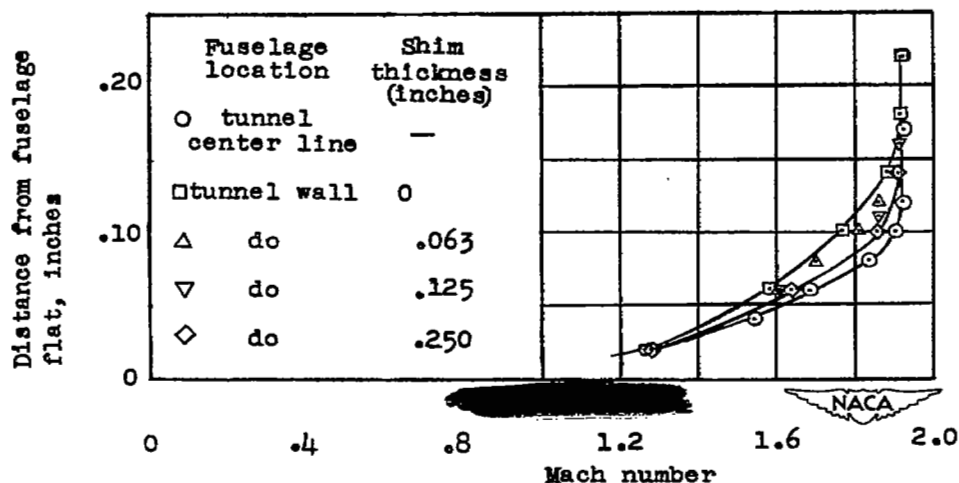
Figure 2.- Concluded.



(a) Arrangement of surface orifices and survey equipment on fuselage.



(b) Pressure distribution along fuselage surface.



(c) Mach number distribution near fuselage.

Figure 3.- Surveys of surface pressure distribution and boundary-layer profile for the fuselage used in the wing tests. Fuselage aligned with the wind stream. $M = 1.9$.

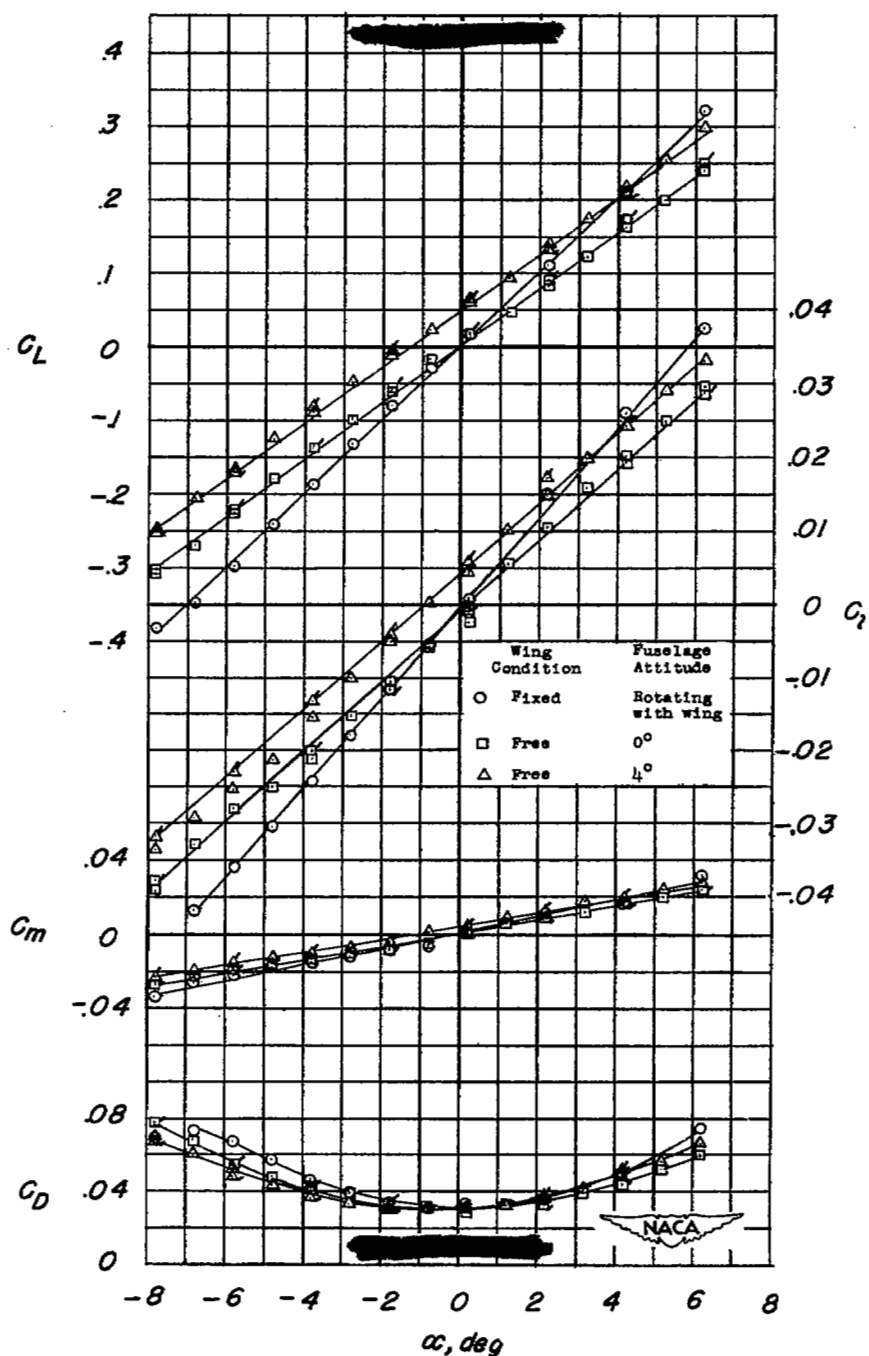


Figure 4.- Aerodynamic characteristics of a half-span trapezoidal wing tested as a fixed and as an all-movable surface in the presence of a half fuselage. $M = 1.9$; $R = 1.4 \times 10^6$. Flagged symbols indicate repeat runs.

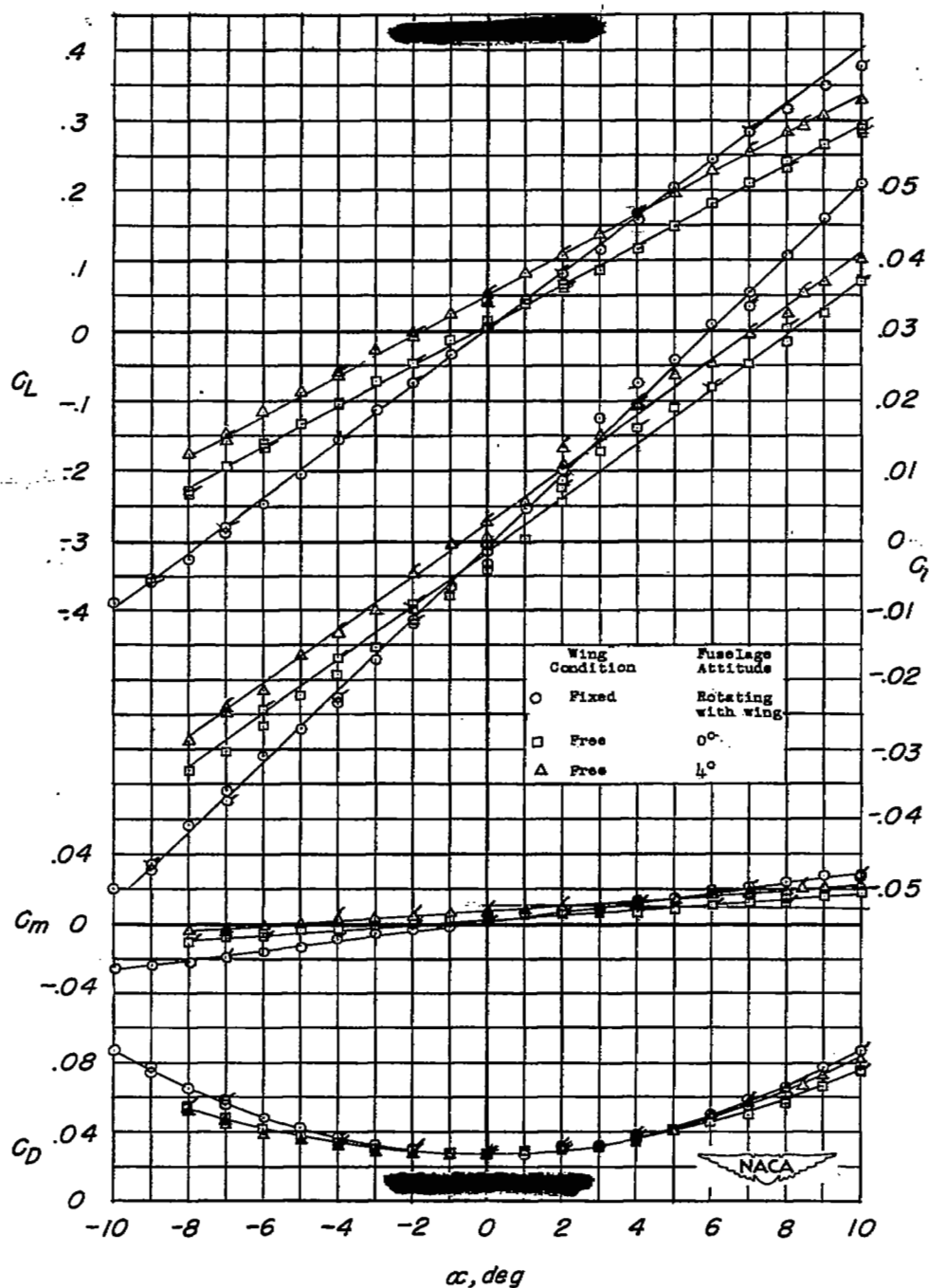
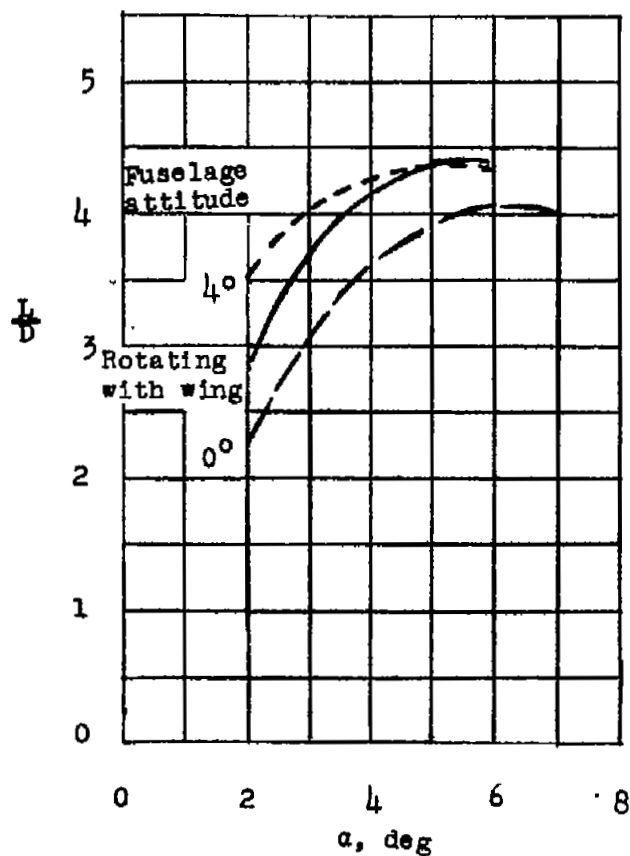
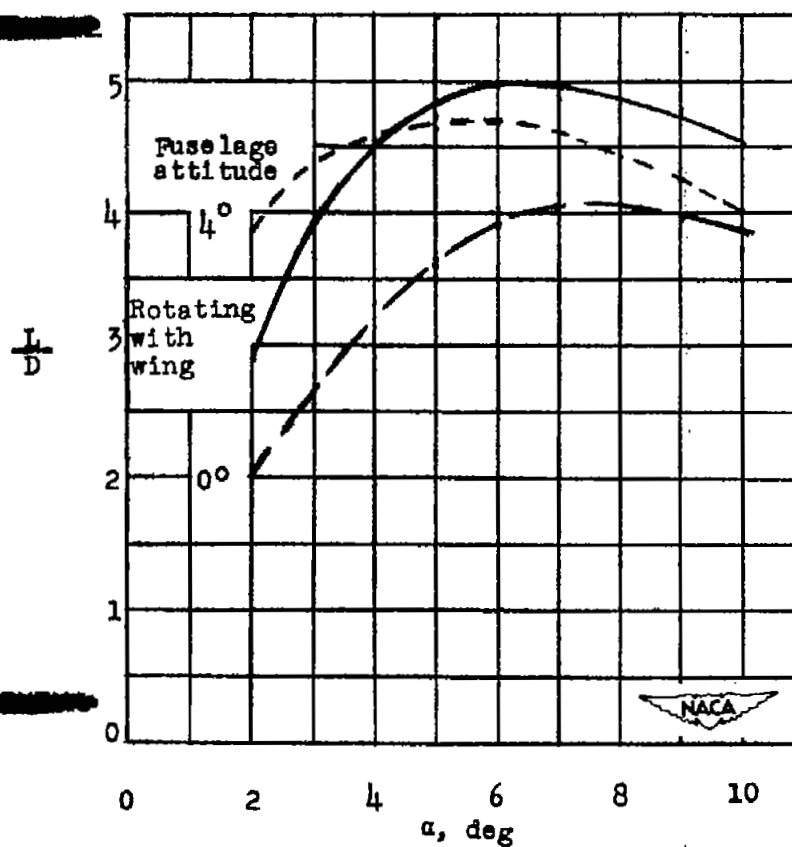


Figure 5.- Aerodynamic characteristics of a half-span delta wing tested as a fixed and as an all-movable surface in the presence of a half fuselage. $M = 1.9$; $R = 1.9 \times 10^6$. Flagged symbols indicate repeat runs.



(a) Trapezoidal wing.



(b) Delta wing.

Figure 6.- Variation of the lift-drag ratio with angle of attack for a half-span trapezoidal and a half-span delta wing. $M = 1.9$.

NASA Technical Library



3 1176 01436 6745